Barlowite: A Spin-1/2 Antiferromagnet with a Geometrically Perfect Kagome Motif

Tian-Heng Han, John Singleton, and John A. Schlueter

Phys. Rev. Lett. **113**, 227203 — Published 25 November 2014

DOI: 10.1103/PhysRevLett.113.227203

Barlowite: a Spin-1/2 Antiferromagnet with Geometrically Perfect Kagome Motif

Tian-Heng Han[1,2†], John Singleton[3], and John A. Schlueter[2,4]
[1] *James Frank Institute and Department of Physics, University of Chicago, Chicago, Illinois 60637, USA*
[2] *Materials Science Division, Argonne National Laboratory, Argonne, Illinois 60439, USA*
[3] *National High Magnetic Field Laboratory, Los Alamos National Laboratory, Los Alamos, New Mexico 87545, USA and*
[4] *Division of Materials Research, National Science Foundation, Arlington, Virginia 22230, USA*
(Dated: September 8, 2014)

We present thermodynamic studies of a new spin-1/2 antiferromagnet containing undistorted kagome lattices—barlowite $Cu_4(OH)_6FBr$. Magnetic susceptibility gives $\theta_{cw} = -136$ K, while long-range order does not happen until $T_N = 15$ K with a weak ferromagnetic moment $\mu < 0.1\ \mu_B$/Cu. A 60 T magnetic field induces a moment less than 0.5 μ_B/Cu at $T = 0.6$ K. Specific heat measurements have observed multiple phase transitions at $T << |\theta_{cw}|$. The magnetic entropy of these transitions is merely 18% of $k_B$ln2 per Cu spin. These observations suggest non-trivial spin textures are realized in barlowite with magnetic frustration. Comparing with the leading spin-liquid candidate herbertsmithite, the superior inter-kagome environment of barlowite sheds light on new spin-liquid compounds with minimum disorder. The robust perfect geometry of the kagome lattice makes charge doping promising.

PACS numbers: 75.50Ee, 75.10Kt, 75.40Cx

Magnetic materials are pervasive in modern physics and quantum mechanics produces unexpected behaviors. A variety of exotic states—many of which are topological—can be hosted in quantum magnets with competing interactions. Knowledge of unconventional magnetism in new compounds has great appeal across boundaries in physics. One of the controversies is whether a quantum spin liquid (QSL), such as a resonating valence bond (RVB) state[1], can be realized experimentally. In a QSL, all the spins result in a long-range quantum entanglement and remain in motion even at a temperature of absolute zero[2]. A QSL cannot be described by broken symmetries in the same way as conventional magnets and represents new states of matter. Having a zoo of exotic phenomena and being a potential key ingredient of high-T_c superconductivity, experimental realizations of a QSL state have been a long and challenging pursue for decades[3,4]. The difficulty is rooted in precisely balancing the microscopic interactions with quantum fluctuations, which together prevent the spins from long-range ordering. Two-dimensional $S = 1/2$ lattices with geometric frustration—where all exchanges cannot be satisfied—are one of the promising protocols. Almost all candidates order magnetically—because of nonstoichiometry issues, imperfect lattice geometries, large spins or perturbing interactions—at low temperatures[5–8], though their ordered spin-textures are complicated and fascinating by themselves.

The leading candidate is the $x = 1$ end member of Zn-paratacamite ($Zn_xCu_{4-x}(OH)_6Cl_2$ with $x > 1/3$) called herbertsmithite[9]. This compound features a geometrically perfect $S = 1/2$ Cu-kagome lattice with a dominating nearest-neighbor Heisenberg antiferromagnetic exchange. As x approaches 1, Cu^{2+} ions at inter-kagome sites are replaced by non-magnetic Zn^{2+} ions. At $x = 1$, the Cu-kagome layers become a two-dimensional magnetic system. Theoretically, the ground state of such a Heisenberg model can be a gapped QSL[10] as well as a gapless one[11,12]. Experimentally, a spinon continuum−fractionalized spin excitations resulting from spin-charge separation−has been observed by neutron scattering, indicating a QSL ground state[9]. However, a precise determination of the stoichiometry of the nominal $x = 1$ sample gives $x = 0.85$[13]. The excess Cu^{2+} ions on the inter-kagome sites weakly couple to the kagome spins through Cu-O-Cu superexchange interactions. This provides additional terms in the spin Hamiltonian and presents challenges to theoretical modeling. In particular, the precise spin Hamiltonian of herbertsmithite remains ambiguous because of the infeasibility for spin wave study. Alternative investigations on clinoatacamite—x = 0 mother compound of herbertsmithite with a magnetically ordered ground state—are devalued due to its Jahn-Teller distorted kagome structure—a ubiquitous conundrum for lattices with spin-1/2 transition metals. At low temperatures or energies, the excess spins have strong response which overwhelms possible smoking-gun evidence of a QSL—the existence/absence of a spin gap[10–12]. In addition to the inter-kagome impurity, a trace amount of Zn^{2+} ions in the Cu-kagome layer remains a nagging concern since these two 3d transition metals are next to each other in the periodic table, though the Zn dilution is measured to be no more than ∼1%[13]. Doping the inter-kagome sites by large non-magnetic Cd^{2+} ions—a 4d transition metal and difficult to exchange sites with Cu—unfortunately distorts the kagome structure and induces spin ordering[14]. For the search of stronger evidence of a QSL, a new family of $S = 1/2$ antiferromagnets featuring undistorted kagome lattces is all the more urgent.

Here we present a new candidate compound, barlowite $Cu_4(OH)_6FBr$[15], with its bulk properties studied using thermodynamic techniques. Barlowite has a hexagonal crystal system in $P6_3/mmc$ space group ($a = 6.6786(2)$ Å, $c = 9.2744(3)$ Å)[16]. As shown in Figs. 1(a) and (b), three Cu^{2+} ions in the formula are crystallographically equivalent and form a geometrically perfect kagome lattice. The space of the inter-kagome site is so large that the fourth Cu^{2+} ion sits in one of three equivalent positions (only the average position is shown). The

TABLE I: Bond angles of the superexchanges in $Cu_4(OH)_6FBr$ at room temperature. Cu1 is in the kagome plane, and Cu2 denotes the average position of three equivalent inter-kagome sites—Cu2a, Cu2b, and Cu2c.

	Cu1-O-Cu1	Cu1-O-Cu2	Cu1-O-Cu2a,b	Cu1-O-Cu2c
angle	117.4°	95.8°	88.7°	107.5°

kagome layers stack on top of each other, different from the staggered stacking in Zn-paratacamite. Barlowite orders magnetically at $T_N = 15$ K and frustrated antiferromagnetism is present with multiple phase transitions at low temperatures. Doping the interlayer sites with large non-magnetic ions is likely to succeed as has been demonstrated in Zn-paratacamite. The kagome spin lattices in barlowite are weakly coupled. As a new mother compound of QSL states, the uniqueness and advantages of barlowite are discussed.

The sample was grown hydrothermally and was characterized by x-ray diffraction[15]. Magnetic susceptibility ($\chi \approx M/H$ in the paramagnetic regime and in the weak-field limit) as a function of temperature has been measured by using a SQUID magnetometer (Quantum Design MPMS) on a 68.5 mg polycrystalline sample—a collection of numerous small crystals. In Fig. 1(c)(inset), the inverse susceptibility is fitted with a Curie-Weiss function for $180 < T < 300$ K. A temperature independence contribution, possibly from the core diamagnetism and the Van Vleck paramagnetism of the sample and the holder, has been subtracted. The Curie-Wiess temperature is $\theta_{cw} = -136 \pm 10$ K, indicating strong antiferromagnetic exchange. The mean-field g factor of the Cu^{2+} ions is 2.27 assuming $S = 1/2$.

Magnetization as a function of field was measured by using an extraction magnetometer[18] in a ^{3}He cryostat. Magnetic fields up to 60 T were provided by a 25-millisecond-duration pulsed magnet at National High Magnetic Field Laboratory at Los Alamos[18]. The magnetometer was calibrated against SQUID measurements, as shown in Fig. 1(d). The low-field behavior is dominated by a hysteresis loop with a coercive field of about 0.01 T (inset). This weak ferromagnetism may be due to the inter-kagome Cu or Dzyaloshinskii-Moriya interaction (DMI). The magnetization jump is less than 0.1 μ_B/Cu, showing that only a small fraction of the available magnetic moment is involved. Above the hysteresis loop, $M(H)$ is monotonic and concave. The polarized moment is 0.48(4) μ_B/Cu at 60 T, corroborating the strong antiferromagnetic exchange. No impurity contribution is observed.

Magnetically, barlowite is better modeled by a stack of weakly coupled kagome layers—instead of a three-dimensional network of tetrahedrons—regarding J'/J, where J' is the exchange between a kagome Cu and the average position for an inter-kagome Cu. Down to $T \sim 0.2\ J/k_B$, the magnetic susceptibility has been calculated, using numerical linked-cluster expansion (NLCE), on a 16-site cluster by considering a kagome lattice coupled to inter-kagome spins[17]. As shown in Fig. 1(c), our susceptibility data is well described by assuming $J'/J = -0.1$ with $J/k_B = -180$ K—slightly less than $\theta_{cw} = -136$ K. In a frustrated magnet, a Curie-Wiess fit

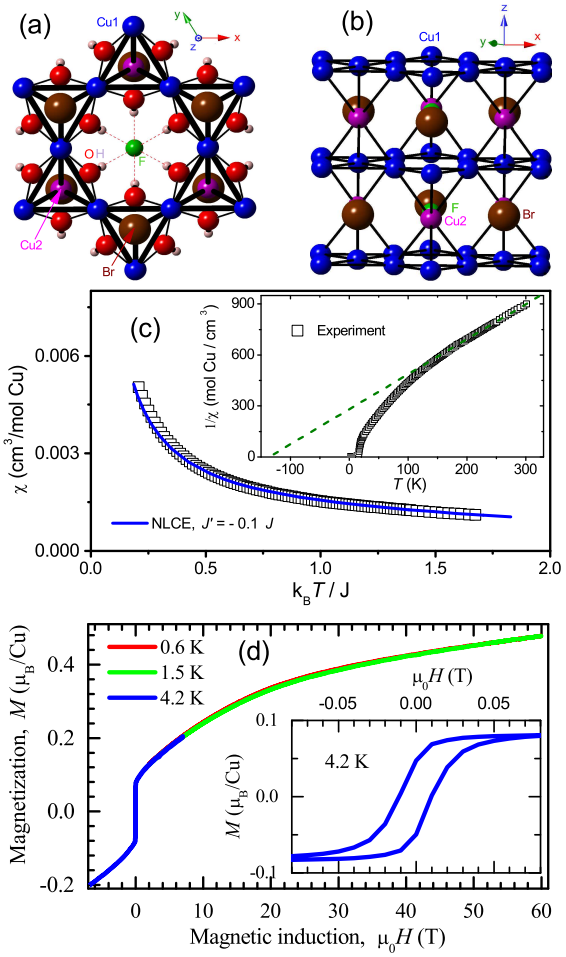

FIG. 1: (color online) Crystal structure of barlowite when looking perpendicular (a) and almost parallel (b) to the kagome lattice. The symbols are: kagome Cu1-blue; inter-kagome Cu2-purple; O-red; H-salmon; F-green; Br-brown. In (a), the thick black lines denote Cu-Cu grids. (c) Magnetic susceptibility of polycrystalline (explained in the text) barlowite measured at $\mu_0 H = 0.1$ T. The data is compared with calculations[17] as described in the text. Inset: inverse susceptibility and a Curie-Weiss fit. (d) Magnetization vs field measured at liquid-helium temperatures. Inset: hysteresis loop at $\mu_0 H < 0.08$ T.

in a temperature range comparable to $|\theta_{cw}|$ often needs to be corrected when quantifying the microscopic exchanges. In addition, θ_{cw} describes the combined effect of all exchanges. As shown in Table. I, J and J' of barlowite are consistent with Goodenough-Kanamori-Anderson rule for the Cu-O-Cu superexchange bond angles[19]. As has been demonstrated in a metal-organic kagome compound, competing antiferromagnetic and ferromagnetic interactions result in a quick saturation of the Cu spin moments at $\mu_B H = J/20$[20]. In herbertsmithite where most of the inter-kagome sites are occupied by non-magnetic Zn^{2+} ions, antiferromagnetic exchange in the kagome lattice dominates, and only 0.1 μ_B/Cu is induced at $\mu_B H = J/3$[21]. Barlowite falls in between with 0.48 μ_B/Cu induced at $\mu_B H = J/2$—consistent with a combined effect from strong in-kagome antiferromagnetic and weak out-of-kagome ferromagnetic exchanges.

Magnetization at low fields is plotted in Fig. 2(a), showing a phase transition to a long-range ordered state with a small ferromagnetic moment at Néel temperature

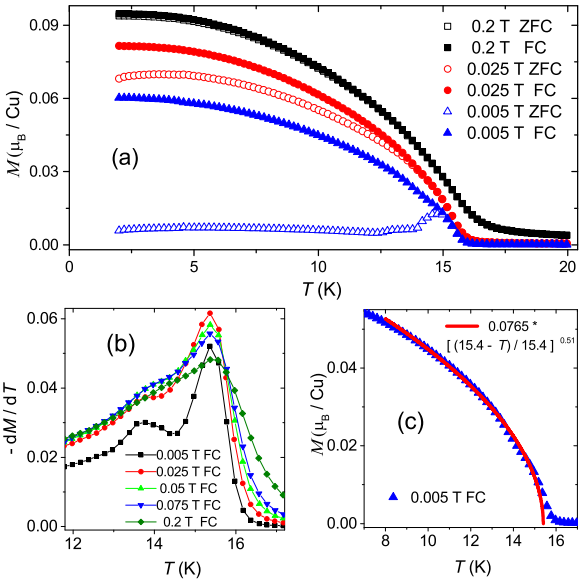

FIG. 2: (color online) Magnetization v.s temperature measured after cooling from room temperature in zero field (ZFC) and a field (FC). (b) Negative derivative of the temperature dependence of magnetization in the proximity of T_N. (c) Power-law fitting to the spontaneous magnetization.

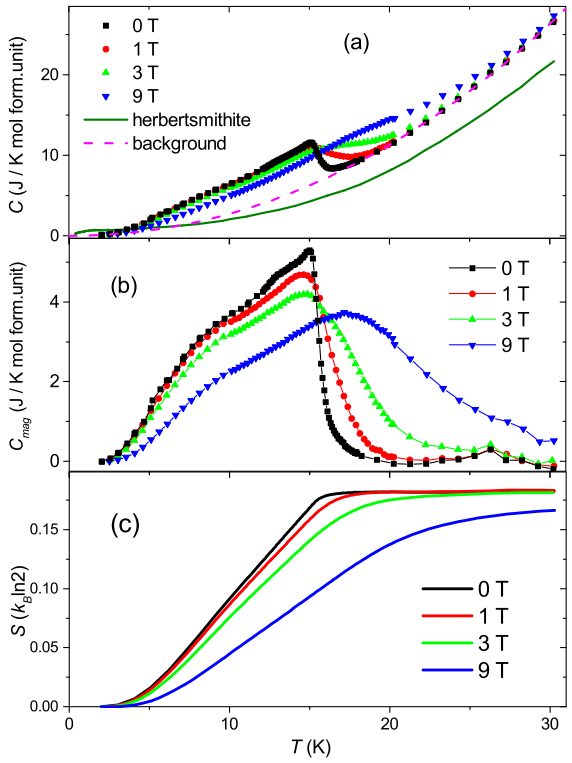

FIG. 3: (color online) (a) Specific heat measured on a single crystal sample of barlowite at fields parallel to the kagome lattice and compared with zero-field specific heat of herbertsmithite[23]. (b) Magnetic specific heat after subtracting the background. (c) Magnetic entropy integrated from T = 2 K and normalized in terms of the total value from the Cu spins.

$T_N = 15.4$ K. At $\mu_0 H = 0.005$ T, zero-field-cooled (ZFC) and field-cooled (FC) data indicate a thermal hysteresis, which gradually vanishes as field increases beyond the coercive field. The thermal hysteresis may originate from domains of the weak ferromagnetism or a trace amount of spin-glass phase, neither of which plays a major role since ZFC and FC curves collapse onto each other at $\mu_0 H = 0.2$ T. In Fig. 2(b), we have plotted the negative derivatives of the FC data shown in Fig. 2(a) in order to precisely detect phase transitions. At $\mu_0 H = 0.005$ T, a second phase transition occurs at $T = 13.8$ K, which broadens at increasing fields and becomes a shoulder of the main peak at 0.2 T. In Fig. 2(c), the spontaneous magnetization below T_N is fitted to a power law $M = At^\beta$ giving $\beta = 0.51$, where $t = |T - T_N|/T_N$ is the reduced temperature and A is a constant. Similar fits at fields up to 0.2 T give β between 0.44 and 0.51. This exponent is larger than 0.39 observed for the three-dimensional ferromagnetic ordering of iron[22]. At $\mu_0 H = 0.005$ T, the ordered moment saturates at 0.06 μ_B/Cu in the $T \to 0$ limit, as shown by the FC curve in Fig. 2(a).

Specific heat was measured using a Quantum Design physical property measurement system (PPMS) on a 5.4 mg single-crystal sample. The field was applied parallel to the kagome plane. In Fig. 3(a), at zero field, a phase transition at $T = 15$ K corroborates the magnetization measurements. The application of a field progressively pushes the entropy below T_N to higher temperatures, indicating that a large part of the low-temperature specific heat is magnetic. A full suppression of the magnetic entropy requires $\mu_0 H > 20$ T. The background specific heat of phonon and disordered spins is estimated by fitting the zero-field specific heat between 20 and 30 K to a polynomial $C_{bg} = aT^2 + bT^3$. The specific heat at $T > 30$ K deviates from a simple polynomial. The returned parameters are $a = 0.0263$ J/K^3 mol form. unit and $b = 9.87 \times 10^{-5}$ J/K^4 mol form. unit. Instead of the T^3 law expected for a lattice structure in 3D, the T^2 term dominates C_{bg}, possibly due to spin correlations formed above T_N. C_{bg} resembles the total specific heat of polycrystalline herbertsmithite with disordered spins. The magnetic specific heat C_{mag} is obtained by subtracting C_{bg} and is shown in Fig. 3(b). As temperature approaches T_N from above at zero field, it is difficult to determine the critical exponent α in $C_{mag} \sim t^{-\alpha}$, since its value depends on C_{bg}. When cooling below T_N, instead of falling towards zero in a power law, a broad hump extends down to $T < 5$ K. A small kink in C_{mag} is seen at $T = 13.8$ K, signaling a second phase transition. For $5 < T < 10$ K, the dome in C_{mag} might indicate slow freezing of the spin moments. At $\mu_0 H = 1$ T, the two closely spaced transitions at T_N and 13.8 K become one rounded peak, which is consistent with the magnetization data in Fig. 2(b). For $T > T_N$, a third phase transition, which is very weak and insensitive to a field of 3 T, takes place at $T = 26$ K. This phase transition has not been observed in magnetization measurements.

Obtained by integrating C_{mag}/T from $T = 2$ to 30 K, Fig. 3(c) shows the magnetic entropy released from the spin ordering transitions. The plateaus at high fields are artifacts from the estimation of C_{bg}. At zero field, the integration gives merely 18% of what is expected for the Cu spins. There is no indication, down to the lowest temperature measured, that residual entropy exists. Apart from the small ordered moments of spin-1/2 ions, the missing entropy may be ascribed to the formation of dynamic spin correlations, such as a chiral spin state[24] or a valence bond solid[25], far above T_N. Such a behavior

is ubiquitous for geometrically frustrated magnets and is also indicated by the deviation from the Curie-Wiess fit at $T < 180$ K in Fig. 1(c). For barlowite, the empirical parameter of frustration $f = |\theta_{cw}|/T_N = 9 >> 1$, indicating the presence of strong frustration[26]. Structurally, it is unclear whether and how the inter-kagome Cu^{2+} ions freeze into one of the three equivalent positions. Such a process releases an entropy of $k_B$ln3 per form. unit, 40% of the total entropy from Cu spins ($4k_B$ln2 per form. unit).

DMI can cause spin canting in a kagome lattice, generating ferromagnetic moments. It also affects the magnetic ground state, possibly tuning it in the proximity of a putative quantum critical point (QCP)[27]. In herbertsmithite, the OH bonds dangle and may freeze randomly at about 50 K, complicating the DMI and spin dynamics[28]. Similarly, in barlowite, J and J' are mediated by OH bonds, and both the in-plane and out-of-plane components of DMI are allowed by symmetry. However, the OH bonds are stabilized because all H^+ ions are connected to F^- ions—through strong hydrogen bonds—between the kagome layers. Since the spin exchanges are sensitive to the hydrogen positions, the HF bond makes possible an accurate determination of the superexchange. It remains unclear how the spinon continuum of herbertsmithite is related to its proximity to a QCP. While resembling many aspects of clinoatacamite and herbertsmithite, the different structure of barlowite provides an opportunity to fine tune the exchange parameters.

Studies on QSL physics largely rely on the reconciliation between experiments and theories[2]. This requires the knowledge of the spin Hamiltonian, which cannot be determined precisely for herbertsmithite in the absence of spin waves[29]. Studies on clinoatacamite may not be helpful since its structure deviates from that of herbertsmithite as a result of Jahn-Teller distortion[30]. In clinoatacamite, θ_{cw} is -190 K and $J' \sim -0.1\,J$[17]. Three magnetic transitions have been observed—two closely spaced at 6 K and one at 18 K[31]. A small ferromagnetic moment $\sim$0.06 μ_B/Cu is observed at $T < 6$ K and μSR measurements support the magnetic nature of the 18 K transition. These properties are similar to those of barlowite. Unfortunately, no neutron scattering experiment has been performed on a single crystal sample and the microscopic spin properties of clinoatacamite remain unknown.

Barlowite sheds light on solutions. Its high structural symmetry relieves crystallographic twinning and allows the growth of large single crystals[32]. Even though the inter-kagome sites are fully occupied by Cu, in contrast to clinoatacamite, barlowite maintains the perfect kagome motif. For neutron scattering experiments, the absorption and incoherent cross sections of deuterated barlowite are much reduced from those of herbertsmithite. This provides an advantage to resolve subtle features at very low energies as well as spin wave dispersions for accurate derivation of the spin Hamiltonian.

The long-range ordering of barlowite at T_N may be suppressed by replacing the inter-kagome Cu with non-magnetic ions. The large space around the inter-kagome site allows many options of 4d transition ions, such as Sn^{2+} or Cd^{2+} ions, paving the way for stoichiometric MCu$_3$(OH)$_6$FBr (M = Sn, Cd, etc) without a concern for antisite disorder. Based on the structure of herbertsmithite, DFT calculation demonstrates the possibility of substituting the inter-kagome Cu with ions of different valence states, modifying the electronic band structure of the kagome lattice[33]. For barlowite, the perfect geometry of the kagome lattice—a core ingredient of QSLs—is extremely robust, making charge doping a real possibility.

In conclusion, a new $S = 1/2$ antiferromagnet containing geometrically perfect kagome layers is realized by barlowite $Cu_4(OH)_6FBr$ with weak out-of-plane ferromagnetic exchanges. Multiple magnetic phase transitions occur at temperatures much lower than the Curie-Weiss temperature, indicating strong frustration and non-trivial spin orders. Single crystals are available for future neutron scattering experiments. By replacing the inter-kagome Cu with non-magnetic ions, new candidates of QSLs will likely emerge with minimum disorder. Regarding the mechanism of high-temperature superconductivity[34], barlowite gives new hope for doping a RVB state.

We thank Patrick Lee, Yasu Takano and Michael Norman for careful reading of the manuscript with useful comments. T.-H. H thanks the support from Grainger Fellowship provided by the Department of Physics, University of Chicago. T.-H. H and J. A. S. thank the supports from Argonne National Laboratory under contract with the Department of Energy (DOE) (DE-AC02-06CH11357). A portion of this work was performed at the National High Magnetic Field Laboratory, which is supported by National Science Foundation Cooperative Agreement No. DMR-1157490, the State of Florida, the DOE and through the DOE Basic Energy Science Field Work Proposal "Science in 100 T". J. S. thanks the University of Oxford for the provision of a visiting professorship. J. A. S acknowledges support from the Independent Research/Development program while serving at the National Science Foundation.

†tianheng@alum.mit.edu

[1] P. W. Anderson, Mat. Res. Bull. **8**, 153 (1973).
[2] L. Balents, Nature **464**, 199 (2010).
[3] P. W. Anderson, Science **235**, 1196 (1987).
[4] P. A. Lee, Science **321**, 1306 (2008).
[5] A. P. Ramirez, G. P. Espinosa, and A. S. Cooper, Phys. Rev. Lett. **64**, 2070 (1990).
[6] M. Yoshida, M. Takigawa, H. Yoshida, Y. Okamoto, and Z. Hiroi, Phys. Rev. Lett. **103**, 077207 (2009).
[7] A. S. Wills, Phys. Rev. B **63**, 064430 (2001).
[8] A. Zorko, F. Bert, A. Ozarowski, J. van Tol, D. Boldrin, A. S. Wills, and P. Mendels, Phys. Rev. B **88**, 144419 (2013).
[9] T.-H. Han, J. S. Helton, S. Chu, D. G. Nocera, J. A. Rodrigues-Rivera, C. Broholm, and Y. S. Lee, Nature **492**,

406 (2012).
[10] S. Yan, D. Huse, and S. White, Science **332**, 1173 (2011).
[11] Y. Iqbal, F. Becca, and D. Poilblanc, Phys. Rev. B **84**, 020407R (2011).
[12] Y. Iqbal, D. Poilblanc, and F. Becca, Phys. Rev. B **89**, 020407R (2014).
[13] D. E. Freedman, T. H. Han, A. Prodi, P. Müller, Q. Z. Huang, Y. S. Chen, S. M. Webb, Y. S. Lee, T. M. McQueen, and D. G. Nocera, J. Am. Chem. Soc. **132**, 16185 (2010).
[14] T. M. McQueen, T. H. Han, D. E. Freedman, P. W. Stephens, Y. S. Lee, and D. G. Nocera, J. Solid State Chem. **184**, 3319 (2011).
[15] See Supplementary Material for more information.
[16] P. Elliott and M. A. Cooper, Mineralogical Magazine **74**, 798 (2010).
[17] E. Khatami, J. S. Helton, and M. Rigol, Phys. Rev. B **85**, 064401 (2012).
[18] P. A. Goddard, T. Lancaster, S. J. Blundell, J. Singleton, P. Sengupta, R. D. McDonald, S. Cox, N. Harrison, F. L. Pratt, J. L. Manson, H. I. Southerland and J. A. Schlueter, New J. Phys. **10**, 083025, (2008).
[19] Y. Mizuno, T. Tohyama, S. Maekawa, T. Osafune, N. Motoyama, H. Eisaki, and S. Uchida, Phys. Rev. B **57**, 5326 (1998).
[20] E. A. Nytko, J. S. Helton, P. Müller, and D. G. Nocera, J. Am. Chem. Soc. **130**, 2922 (2008).
[21] T.-H. Han, R. Chisnell, C. J. Bonnoit, D. E. Freedman, V. S. Zapf, N. Harrison, D. G. Nocera, Y. Takano, and Y. S. Lee, arXiv:1402.2693 (2014).
[22] S. Arajs, B. L. Tehan, E. E. Anderson, and A. A. Stelmach, Phys. Lett. **32A**, 412 (1970).
[23] J. S. Helton, K. Matan, M. P. Shores, E. A. Nytko, B. M. Bartlett, Y. Yoshida, Y. Takano, A. Suslov, Y. Qiu, J.-H. Chung, D. G. Nocera and Y. S. Lee, Phys. Rev. Lett. **98**, 107204, (2007).
[24] D. Grohol, K. Matan, J.-H. Cho, S.-H. Lee, J. W. Lynn, D. G. Nocera, and Y. S. Lee, Nat. Mater. **4**, 323 (2005).
[25] K. Matan, T. Ono, Y. Fukumoto, T. J. Sato, J. Yamaura, M. Yano, K. Morita, and H. Tanaka, Nat. Phys. **6**, 865 (2010).
[26] A. P. Ramirez, Annu. Rev. Mater. Sci **24**, 453 (1994).
[27] O. Cëpas, C. M. Fong, P. W. Leung, and C. Lhuillier, Phys. Rev. B **78**, 140405(R) (2008).
[28] T. Imai, E. A. Nytko, B. M. Bartlett, M. P. Shores, and D. G. Nocera, Phys. Rev. Lett. **100**, 077203 (2008).
[29] T. Han, S. Chu, and Y. S. Lee, Phys. Rev. Lett. **108**, 157202 (2012).
[30] P. Mendels and F. Bert, J. Phys. Soc. Japan **79**, 011001 (2010).
[31] X. G. Zheng, T. Kawae, Y. Kashitani, C. S. Li, N. Tateiwa, K. Takeda, H. Yamada, C. N. Xu, and Y. Ren, Phys. Rev. B **71**, 052409 (2005).
[32] T. H. Han, J. S. Helton, S. Chu, A. Prodi, D. K. Singh, C. Mazzoli, P. Müller, D. G. Nocera, and Y. S. Lee, Phys. Rev. B **83**, 100402R (2011).
[33] I. I. Mazin, H. O. Jeschke, F. Lechermann, H. Lee, M. Fink, R. Thomale, and R. Valenti, Nat. Commun. **5**, 4261 (2014).
[34] P. A. Lee, N. Nagaosa, and X.-G. Wen, Rev. Mod. Phys. **78**, 17 (2006).